

Fabrication of small superconducting coils using $(\text{Ba},A)\text{Fe}_2\text{As}_2$ (A : Na, K) round wires with large critical current densities

Sunseng Pyon¹, Haruto Mori¹, Tsuyoshi Tamegai¹, Satoshi Awaji², Hijiri Kito³, Shigeyuki Ishida³, Yoshiyuki Yoshida³, Hideki Kajitani⁴, Norikiyo Koizumi⁴

¹Department of Applied Physics, The University of Tokyo, Bunkyo, Tokyo 113-8656, Japan

²High Field Laboratory for Superconducting Materials, Institute for Materials Research, Tohoku University, Sendai 980-8577, Japan

³Research Institute for Advanced Electronics and Photonics, National Institute of Advanced Industrial Science and Technology, Tsukuba, Ibaraki 305-8568, Japan

⁴Naka Fusion Institute, National Institutes for Quantum and Radiological Science and Technology (QST), 801-1 Mukoyama, Naka-shi, Ibaraki 311-0193, Japan

Abstract

We report the fabrication of small $(\text{Ba},A)\text{Fe}_2\text{As}_2$ (A : Na, K) coils using 10 m-class long round wires, fabricated by powder-in-tube (PIT) method. Coils are sintered using hot-isostatic-press (HIP) technique after glass-fiber insulations are installed. Critical current (I_c) of the whole coil using $(\text{Ba},\text{Na})\text{Fe}_2\text{As}_2$ and $(\text{Ba},\text{K})\text{Fe}_2\text{As}_2$ are 60 A and 66 A under the self-field, and the generated magnetic fields at the center of the coil reach 2.6 kOe and 2.5 kOe, respectively. Furthermore, the largest transport critical current density (J_c) and I_c in $(\text{Ba},\text{Na})\text{Fe}_2\text{As}_2$ wires picked up from the coil reach 54 kAcm^{-2} and 51.8 A at $T = 4.2 \text{ K}$ under a magnetic field of 100 kOe, respectively. This value exceeds transport J_c of all previous iron-based superconducting round wires. Texturing of grains in the core of the wire due to the improvement of the wire drawing process plays a key role for the enhancement of J_c .

Keywords: iron-based superconductor, HIP round wires, superconducting coil, critical current, critical current density, $(\text{Ba},\text{Na})\text{Fe}_2\text{As}_2$, $(\text{Ba},\text{K})\text{Fe}_2\text{As}_2$

Introduction

Iron-based superconductors (IBSs) are expected to be the next generation high temperature superconductors for high magnetic field applications. Among IBSs, 122-type compounds such as $(AE,A)Fe_2As_2$ ($AE = Ba, Sr, A = Na, K$) are considered to be promising materials for practical use. Both critical temperature T_c (< 38 K) [1-6] and upper critical field H_{c2} (> 650 kOe) [2,7-9] of $(AE,A)Fe_2As_2$ are larger than those of practically used NbTi and Nb₃Sn. Compare with MgB₂ with similar T_c (~ 39 K) [10], which is developed to be used for MRI, H_{c2} is much larger. Small anisotropy $\gamma < 2$ [7-9] and large critical grain boundary angle of $\sim 9^\circ$ for critical current density (J_c) in $(AE,A)Fe_2As_2$, which is larger than that of $\sim 5^\circ$ in cuprate YBa₂Cu₃O_{7- δ} [11], suggest that high and three-dimensional texturing is not necessary unlike tapes and coated conductors of cuprates. So the IBSs are suitable for applications such as superconducting wires, tapes, and coated conductors. Furthermore, robustness of J_c under high magnetic fields in IBSs is also preferred for high-field applications. In $(AE,K)Fe_2As_2$ single crystal, large J_c above 1 MAcm⁻² below 5 K at self-field has been demonstrated. Furthermore, values of J_c can be increased by adding pinning center by ion-irradiation [12-16]. Superconducting wires and tapes fabricated by powder-in-tube (PIT) method using polycrystalline $(AE,K)Fe_2As_2$ powders have been also studied [17-24]. Transport J_c of wires and tapes can be increased by purification of raw materials [25] and densification of the core [26] to eliminate weak links between superconducting grains. To enhance J_c by densification of superconducting core, pressing at high temperature is effective for IBS wires. Uniaxial hot press technique has been applied for textured tapes [26-36]. On the other hand, hot isostatic press (HIP) methods has been applied for round wires [15,37-49]. The transport J_c under a high field of 100 kOe at 4.2 K for tapes of $(Ba,K)Fe_2As_2$ has reached 150 kAcm⁻², which exceeds the practical level of 100 kA cm⁻² [31]. In the case of tapes, transport J_c is significantly enhanced by texturing of the grains due to their flat shapes helped by uniaxial pressing [26,44]. In the case of round wires, which are suitable for winding coils, texturing of the grains is difficult compared with that in tapes. However, it has been demonstrated that the degree of texturing of the grains can be enhanced to a certain degree by changing deformation process, leading to larger J_c [44]. The transport J_c under a high field of 100 kOe at 4.2 K for wires of $(Ba,K)Fe_2As_2$ and $(Ba,Na)Fe_2As_2$ have reached at levels of 38 and 44 kAcm⁻², respectively.

For practical applications of these promising wires and tapes, further important progresses, such as fabrication of wires with multifilament core [28,50,51] and superconducting joints [52,53], have been reported. One of the most typical applications of superconducting wires and tapes is the fabrication of coils to generate magnetic fields. In 2017, fabrications of 100 m-class $(Sr,K)Fe_2As_2$ tapes and coils using these tapes were reported for the first time, although generated magnetic field was not reported [54]. Recently, using $(Ba,K)Fe_2As_2$ tapes, fabrications of several coils and evaluation of critical current I_c have been reported [55-57]. For example, the transport I_c of the

pancake coil achieved 35 and 25 A under magnetic fields of 100 and 240 kOe at 4.2 K, respectively [55]. A racetrack coil was also fabricated, and it quenched at 100 kOe at 4.2 K near the operating current of 65 A, which is as large as 86.7% of I_c of the short sample at the same condition [57]. These results clearly indicate that IBSs are very promising for high-field magnet applications. On the other hand, there have been few reports on IBS round wires longer than 1 m or a coil using round wires. Furthermore, not much attention has been paid to I_c of round wires, although there have been several reports on J_c of the wire. Very recently, relatively large I_c in short pieces of round wires, and the fabrication of a small demo coil using round wires with length up to 9 m has been reported [58]. I_c in a short piece of the wire under the magnetic field of 10 or 100 kOe at 4.2 K are 95 or 54 A, respectively. $I_c \sim 54$ A at 100 kOe corresponds to $J_c \sim 42$ kAcm⁻², which is comparable to the largest value of J_c in round wires (44 kAcm⁻²) in previous reports [48,49]. A small demo coil, fabricated without insulation, generated 1.5 kOe at 60 A at 4.2 K, which was smaller than the expected value [58]. In addition, the magnetic field shows appreciable time dependence with a long time constant due to no insulation. These results suggest that there is a lot of room for improvements of coil fabrications with IBS round wires. In the case of MgB₂, coils using superconducting PIT wire have been studied [59,60]. Using a 58 m-long PIT wire, a superconducting magnet was fabricated, which generated a magnetic field of 19 kOe at 4.2 K [60]. Demonstration of generating magnetic field using IBS coil is also demanded.

In this report, we demonstrate the fabrication of small coils using 10 m-class long round wires of (Ba,Na)Fe₂As₂ and (Ba,K)Fe₂As₂. Round wires are fabricated by PIT method. Coils are wound by using long wires covered by insulating fiber-glass sleeves, then sintered using HIP technique. Generated magnetic field of the coils and their I_c are also evaluated. Furthermore, largest transport J_c in the short segment picked up from the (Ba,Na)Fe₂As₂ coil reached 54 kAcm⁻² at $T = 4.2$ K under a magnetic field of 100 kOe. This value exceeds the value of transport J_c of all previous IBS round wires. Details of the fabrication and characterization of wires and coils, and characterizations of short segments of the wire picked up from the coils including X-ray diffraction (XRD) and X-ray computed tomography (CT) are shown and discussed.

Experimental methods

(Ba,Na)Fe₂As₂ and (Ba,K)Fe₂As₂ round wires were fabricated by *ex situ* PIT method. Polycrystalline powders of (Ba,Na)Fe₂As₂ and (Ba,K)Fe₂As₂ were synthesized by solid state reaction after mixing the raw materials of elements by ball milling method. Details of synthesis are described in Ref. [48] and Ref. [42]. It should be noted that raw materials of (Ba,K)Fe₂As₂ before synthesis were accidentally exposed to a little amount of air, which may affect the results on (Ba,K)Fe₂As₂ wire and coil as described below. After grinding by agate motor in Ar atmosphere, polycrystalline powder was filled into a Ag tube with outer diameter (OD) and inner diameter (ID) of 4.5 mm and 3 mm,

respectively. The Ag tube filled with the polycrystalline powder was cold-drawn successively using dies with circular holes down to a diameter of ~ 1.9 mm. Obtained wires were inserted into Cu tubes with OD and ID of 3.0 mm and 2.0 mm, respectively. It should be noted that we used Cu tubes with different outer and inner diameters compared with previous reports (OD and ID of 3.2 mm and 1.6 mm) to increase I_c of the wire by enhancing the cross-sectional core area [44,48]. They were cold-drawn using dies with circular holes, and formed into a round shape with a diameter of ~ 2.3 mm (~ 2.6 mm) for $(\text{Ba,Na})\text{Fe}_2\text{As}_2$ ($(\text{Ba,K})\text{Fe}_2\text{As}_2$). Then, the tube was swaged using a rotary swaging machine, and formed into a round shape with a diameter of 1.0 mm (1.16 mm) for $(\text{Ba,Na})\text{Fe}_2\text{As}_2$ ($(\text{Ba,K})\text{Fe}_2\text{As}_2$). The total lengths of long wires reach ~ 12.5 m and ~ 10 m for $(\text{Ba,Na})\text{Fe}_2\text{As}_2$ and $(\text{Ba,K})\text{Fe}_2\text{As}_2$ wires, respectively. For insulation of the long wires, fiber-glass sleeves were installed, which increased the total diameter of the wire to ~ 1.3 mm. Then, they were wound around stainless steel bobbins, and fixed by being tied up with fiber-glass sleeves. After sealing the edges of wires by an arc welder, coils were sintered at 700°C for 4 h using the HIP technique. HIP processes for $(\text{Ba,Na})\text{Fe}_2\text{As}_2$ and $(\text{Ba,K})\text{Fe}_2\text{As}_2$ coils were performed under 200 MPa at National Institute of Advanced Industrial Science and Technology and under 190 MPa at National Institutes for Quantum and Radiological Science and Technology, respectively. The I_c of the coils under the self-field and generated magnetic field at the center of coils were measured at The University of Tokyo. In order to minimize the effect of Joule heating at the current leads, measurements were performed in liquid helium. Current–voltage (I – V) characteristics were measured by the four-probe method with solder for contacts, which were made at ends of the wires for coils. The generated magnetic field at the center of the coil was measured using a Hall probe (THS126, Toshiba). After evaluation of properties of coils, short segments of wires were picked up from coils at every 1 m distance from the end. I_c of the short segments of the wire from $(\text{Ba,Na})\text{Fe}_2\text{As}_2$ coil were measured in static magnetic field up to 140 kOe using the 15T-SM at the High Field Laboratory for Superconducting Materials, IMR, Tohoku University. Similar measurements on short segments of the wire from $(\text{Ba,K})\text{Fe}_2\text{As}_2$ coil under the self-field were performed at The University of Tokyo. For the X-ray CT imaging of short segments of wires from $(\text{Ba,Na})\text{Fe}_2\text{As}_2$ and $(\text{Ba,K})\text{Fe}_2\text{As}_2$ coils, we used Carl Zeiss METROTOM 1500 with setting 200 kV for X-ray tube voltage or SMX-160CT-SV3 (Shimadzu corporation) with setting 160 kV for X-ray tube voltage, respectively. The bulk magnetization of a short piece of the wire was measured to characterize the superconducting transition and magnetic J_c by a superconducting quantum interference device magnetometer (MPMS-5XL, Quantum Design). Vickers hardness, HV [61], was measured on the polished surface of the wire core. Powder XRD with Cu-K α radiation (Smartlab, Rigaku) for the polycrystalline powders and the core of the wires were carried out for the evaluation of texturing of the core of the wires.

Experimental results and discussion

Photos of small superconducting coils fabricated from (Ba,Na)Fe₂As₂ and (Ba,K)Fe₂As₂ wires are shown in Figs. 1(a) and (b), respectively. Specifications of wires and coils including geometrical dimensions and I_c are summarized in Table 1. The I - V characteristics and current dependence of generated magnetic field of the (Ba,Na)Fe₂As₂ and (Ba,K)Fe₂As₂ coils are shown in Figs. 2(a) and 2(b), respectively. As shown in Fig. 2(a), when the current is smaller than ~60 A, a linear increase of the voltage is observed, which amounts to the resistance of ~1 mΩ in the (Ba,Na)Fe₂As₂ coil. This finite resistance originates from the resistance of Cu wire without superconducting core at ends of the wire with a total length of ~10 cm, which we found out later. We evaluated the transport I_c for coils by adopting the 1 μVcm⁻¹ criterion after subtract the linear component originated from the resistance of Cu. Then I_c of the (Ba,Na)Fe₂As₂ coil can be estimated as ~60 A at 4.2 K under the self-field. The generated magnetic field increases linearly as a function of the current both below and above I_c as expected. This indicates that insulation of the wound wire works effectively, in contrast to the coil without insulation in the previous report [58]. At 60 A, generated magnetic field reaches 2.6 kOe, which corresponds to the coil constant of the (Ba,Na)Fe₂As₂ coil of ~43 Oe/A. Similarly, as shown in Fig. 2(b), the (Ba,K)Fe₂As₂ coil generated 2.5 kOe at I_c of 66 A, which corresponds to the coil constant of ~38 Oe/A. A linear increase of the voltage is also observed in the (Ba,K)Fe₂As₂ coil by the same reason. The magnetic field at the center of a coil with finite dimensions can be calculated using the following formula [62];

$$H = \frac{\mu_0 N I}{2(R_2 - R_1)} \ln \frac{R_2 + \sqrt{R_2^2 + l^2}}{R_1 + \sqrt{R_1^2 + l^2}},$$

where μ_0 is vacuum permeability, N is the numbers of turns, $2l$ is the height of the coil along its axis, $2R_1$ and $2R_2$ are ID and OD of the coil, respectively. Values of these parameters are also summarized in Table 1. The calculated coil constants of 41 Oe/A and 39 Oe/A, H/I , are close to the measured coil constants of 43 Oe/A and 38 Oe/A for the (Ba,Na)Fe₂As₂ and (Ba,K)Fe₂As₂ coils, estimated from the slope of H - I graphs in Figs. 2(a) and 2(b), respectively. These results indicate that both (Ba,Na)Fe₂As₂ and (Ba,K)Fe₂As₂ coils are properly fabricated as designed.

After the characterization of generated magnetic field, wires of the coils were unwound and short segments of wires were picked up at every 1 m from the end, and they were evaluated. Figs. 3(a) and 3(b) exhibit I_c of these short segments of wires from (Ba,Na)Fe₂As₂ and (Ba,K)Fe₂As₂ coils, respectively. We evaluated the transport I_c for short segments of the wires by adopting the 1 μVcm⁻¹ criterion. As shown in Fig. 3(a), I_c varies considerably along the length of the (Ba,Na)Fe₂As₂ wires. The maximum values of I_c of (Ba,Na)Fe₂As₂ wires reach 168, 104, and 51.8 A at 0, 10, and 100 kOe, respectively, for a segment at 4 m from the end of the wire. On the other hand, I_c under the self-field varied between 80 A and 170 A for segments between 0 m and 10 m from the end. Such a large variation of I_c suggests the presence of small cracks or inhomogeneities in the superconducting core

in the 10-m class long wire wound in the coil. It should be noted that transport J_c of the IBS wire can be underestimated by accidental presence of micro cracks in the superconducting core. Empirically, values of transport I_c is distributed roughly in the range of 70~100%, when several pieces of wires fabricated in the same process are measured. Furthermore, in the present study, wires were picked up after unwinding from the coil. Obviously, unwinding process can introduce small cracks. Considering these effects, I_c variation can be explained. Furthermore, the segments at 11 m and 12 m from the end shows significantly small I_c below 22 A. This may be caused by accidental stress applied during the unwinding process. These inhomogeneities and partial damage in the wire of the coil cause the relatively smaller I_c of ~60 A of the (Ba,Na)Fe₂As₂ coil compared with the largest I_c of ~170 A for short segments. In the case of short segments picked up from the (Ba,K)Fe₂As₂ coil, values of I_c varied between 60 A and 110 A. The maximum I_c of short segments picked up from the (Ba,K)Fe₂As₂ coil is smaller than that from (Ba,Na)Fe₂As₂ coil, although the cross sectional area of superconducting core of (Ba,K)Fe₂As₂ is similar to that of (Ba,Na)Fe₂As₂. However, details inspections of the (Ba,K)Fe₂As₂ wire show the presence of inhomogeneities as shown below. The minimum I_c of ~60 A is comparable to the I_c of ~66 A of the (Ba,K)Fe₂As₂ coil.

To further characterize the wire, optical micrographs of the cross section and X-ray CT images are taken for short segments of (Ba,Na)Fe₂As₂ and (Ba,K)Fe₂As₂ wires. Both optical and CT images of the transverse cross section of wires are shown in Figs. 4(a), (d), and Figs. 4(b), (e), respectively, showing nearly circular shapes of wires and isotropic shapes of superconducting cores, which were fabricated by drawing using dies with circular holes and swaging using a rotary swaging machine. Longitudinal cross sections of wires were also observed by X-ray CT as shown in Figs. 4(c) and 4(f). Some degrees of sausageing of the superconducting core can be observed in (Ba,Na)Fe₂As₂ wire, while the core is nearly homogeneous in (Ba,K)Fe₂As₂ wire. It should be noted that transport I_c are not overestimated due to the fluctuation of the longitudinal cross section area. In principle, the value of transport I_c can be determined by the minimum cross section area of the core between two voltage terminal. The distance between two voltage terminals for measurements of I_c is 5~10 mm. As is observed in the X-ray CT images of Fig. 4, the period of sausageing of the core of the wire is shorter than that distance. We cut the wire 10~20 mm away from the terminal to evaluate the area of cross section of the wire for the evaluation of transport J_c . This randomly chosen cross sectional area of the core is always equal to or larger than the minimum area of the wire core. So, at least, the value of transport J_c is not be overestimated. It should be noted that, as shown in Fig. 4(d), numerous black dots can be observed in the superconducting core of the wire picked up from the (Ba,K)Fe₂As₂ coil. They are voids in the core or KOH attached on the surface of the core. Existence of KOH suggests two possibilities. First, KOH just exist as an impurity phase in the core. Second, unreacted K in the superconducting core reacted with moisture in the air. These impurities are mainly caused by accidental exposure of raw materials to air for a few seconds as described above. By contrast, such

black dots are not observed in the superconducting core of (Ba,Na)Fe₂As₂ wire as shown in Fig. 4(a). Presence of voids and residual KOH explain the smaller I_c in short segments picked up from the (Ba,K)Fe₂As₂ coil compared with that from the (Ba,Na)Fe₂As₂ coil.

After the evaluation of the area of superconducting core of short segments of the wire from (Ba,Na)Fe₂As₂, it is found that the value of transport J_c at high magnetic field of 100 kOe exceeds the record value of all IBS round wires. The magnetic field dependence of the transport J_c (I - V) and magnetic J_c (M - H) at 4.2 K for the wires picked up from the (Ba,Na)Fe₂As₂ coils are shown in Figs. 5(a) and (b), respectively. Transport and magnetic J_c in the (Ba,Na)Fe₂As₂ HIP wire, which were the largest values of J_c in IBS round wires, from our previous publication are also plotted [49]. As shown in Fig. 5(a), transport J_c under the magnetic field of 10 and 100 kOe of the wires picked up from the (Ba,Na)Fe₂As₂ coil at 4 m (7 m) reach 109 (114) and 54 (52) kAcm⁻², respectively. The transport J_c of 54 kAcm⁻² under 100 kOe at 4.2 K is more than 20% larger than the previous largest value of J_c of 44 kAcm⁻² [49]. Larger J_c compared with that in the previous report can be observed in the whole magnetic field range as shown in Fig. 5(a). The magnetic J_c of the same wires plotted in Fig. 5(b) were evaluated from the irreversible magnetization using the extended Bean model [12], $20\Delta M/a(1-a/3b)$, where $\Delta M(\text{emu/cm}^3)$ is $M_{\text{down}} - M_{\text{up}}$. M_{up} and M_{down} are the magnetization when sweeping the field up and down, respectively, and $a(\text{cm})$ and $b(\text{cm})$ are the lateral dimensions of the core, approximated by a rectangle ($a < b$), keeping the same area of the actual core. Magnetic field is applied parallel to the current flow direction for the wire. Thickness of the sample for the evaluation of magnetic J_c is ~0.5 mm. Fluctuation of the area of cross section is not so large as shown in X-ray CT images of Fig. 4. Furthermore, we also checked both cross sectional areas of the core are comparable. So the fluctuation of cross section area of the cores does not affect the evaluation of magnetic J_c . As shown in Fig. 5(b), magnetic J_c under the self-field and 40 kOe of the wires picked up from the (Ba,Na)Fe₂As₂ coil at 4 m (7 m) from the end reach 372 (387) and 67 (66) kAcm⁻², respectively. The magnetic J_c near the self-field are more than twice larger than the transport J_c , while J_c values evaluated by two methods are comparable at higher magnetic fields. Compared with the previous data shown in Fig. 5(b), the magnetic J_c of the present wire is larger in the whole magnetic field range. On the other hand, both transport and magnetic J_c of the short segments of the wire picked up from the (Ba,Na)Fe₂As₂ coil at 11 m from the end are significantly smaller than those of other wires. As described above, this may be caused by accidental stress applied during the unwinding process. On the other hand, quality of short segments cut from (Ba,K)Fe₂As₂ coil is worse. In Fig. 6, both transport and magnetic J_c of some short segments cut from (Ba,K)Fe₂As₂ coils are shown. Compared with the previous value in Ref. [44], the highest J_c among all (Ba,K)Fe₂As₂ round wires, values of both transport and magnetic J_c are about half of the previous values. This inferior performance should be caused by the accidental exposure of raw materials to air as described above. The present study demonstrates that a part of short segments of the wire picked up

from the (Ba,Na)Fe₂As₂ coil shows the transport J_c of 54 kAcm⁻² at 100 kOe, which is larger than the previous record of IBS round wires of 44 kA cm⁻² [48,49], as shown in Fig. 5(a). One of possible key factors for the enhancement of J_c is the quality of polycrystalline powder. To confirm this, characteristics of (Ba,Na)Fe₂As₂ powders used in this work and in the previous work in Ref. [48] are compared. Temperature dependence of normalized magnetization of two kinds of (Ba,Na)Fe₂As₂ powders are shown in Fig. 7(a). The onset T_c of ~35 K in both powders are almost the same, although the drop of magnetization near T_c in the powder used in the present work is sharper than that in the previous work. On the other hand, T_c and sharpness of the drop of magnetization near T_c are comparable for both wires fabricated in the present work and in the previous report [49], as shown in Fig. 7 (b). In the case of superconducting cores in sintered wires at high pressure, subtle changes of magnetization due to the presence of lower T_c phases can be hidden behind the large shielding effect of the main body. Still a little bit higher quality of polycrystalline powder in the present study helped to enhance transport J_c . Next, texturing in the superconducting core may also play a key role for the enhancement of J_c , as discussed for IBS round wires [44,48,49]. It is reported that the degree of texturing of the grains in the core is affected by the method how the wire was drawn [44]. In the present study, long wires for the coils were fabricated using dies with circular holes and a rotary swaging machine, resulting in nearly circular cross section. By contrast, the Cu-Ag-sheathed wires in previous reports were drawn into a square shape with a groove roller at the final stage, although Ag-sheathed wires before packing into Cu tube were drawn by using dies with circular holes [44,48,49]. More isotropic circular cross section compared with the rectangular shape may be more advantageous for the texturing of grains. In order to confirm possible texturing in the core of (Ba,Na)Fe₂As₂ round wires, we performed the XRD measurements. Figure 8(a) shows (002) and (103) peaks from longitudinal cross sections of the wire picked up from the (Ba,Na)Fe₂As₂ coil at 4 m from the end with transport J_c at 100 kOe of 54 kAcm⁻². The relative intensity of (002) peaks compared with that of (103), defined by $r = I(002)/I(103)$, for this wire is ~0.36. The values r of other (Ba,Na)Fe₂As₂ HIP wires have good correlation with transport J_c at 100 kOe. Namely, r values for wires with $J_c(100 \text{ kOe}) = 34, 40, \text{ and } 44 \text{ kAcm}^{-2}$ are ~0.20, ~0.27, and ~0.33, respectively [49]. The value of r is a good parameter for concentric texturing of grains in the core around the long axis of the wire, and it should have a positive effect on the enhancement of J_c . We also performed a similar measurement for another part of the segment. As shown in Fig. 8 (b), r value of the wire, picked up from the (Ba,Na)Fe₂As₂ coil at 1 m from the end, is ~0.35, comparable to the value for another segment. This result suggests that the degree of texturing of grains is homogeneous in the whole coil although I_c have some variation due to micro cracks. We also performed the HV measurement for the same wire. The HV of the present wire is 253 [kgfmm⁻²], which is slightly larger than that of 247 [kgfmm⁻²] in previous report [49]. It was reported that high densification of the core of wires or tapes, which can reduce weak links between superconducting grains, can also

help to enhance J_c [26]. Although wires in the present and previous studies were sintered at the same pressure of 200 MPa, the thickness of Cu sheath, shapes of the cross section of the wire (rectangle or circle), and the diameter of the wire are different from each other. These differences may affect HV of the wires. From these results, we speculate that texturing of the grains mainly affect for enhancement of transport J_c at high magnetic field, while higher quality of powders and higher densification of the core also contribute to that.

In the present study, we demonstrate the fabrication of both $(\text{Ba,Na})\text{Fe}_2\text{As}_2$ and $(\text{Ba,K})\text{Fe}_2\text{As}_2$ coils, which generated magnetic field of 2.6 and 2.5 kOe, and have I_c of 60 and 66 A, respectively. Here we discuss strategy for further enhancement of generated magnetic field using IBS coils. Figure 9 shows the load line and I_c of the $(\text{Ba,Na})\text{Fe}_2\text{As}_2$ coil together with the I_c - H curve of the short segment picked up from the coil at 4.2 K. I_c at the intersection of the load line and field dependence of I_c of the short segment is ~ 140 A, which is more than twice as large as that of the coil. The suppression of J_c of the coil is due to the inhomogeneities and partial damage in the wound wire as discussed above. Improvements of the fabrication process for good uniformity of current carrying capability for the whole length of the wire are demanded. Load line and field dependence of I_c of the short segment in Fig. 9 suggests that increase of I_c and/or enhancement of the coil constant should be needed to generate magnetic field higher than 10 kOe. The area of cross section of the superconducting core was increased by changing the dimensions of Cu sheath compared with the previous reports [44,48,49]. However, as shown in Fig. 4, the fraction of the superconducting core is still small. The diameter of the wire is more than 2.5 times larger than that of the core. There is still much room for expanding the area of the core by reducing thickness of metal sheaths. Coil constants of the fabricated test coil were 38-43 Oe/A as described in Table 1. According to the formula for the generated magnetic field of the coil, coil dimensions $2l$ and $2R_2$ should be increased to generate higher magnetic field. Furthermore, longer wire is necessary. As described above, the I_c at 10 kOe of the short segments of the wires is ~ 100 A. So the coil constant should be increased larger than 100 Oe/A to generate a magnetic field higher than 10 kOe. As an example, the coil constant becomes ~ 100 Oe/A, when N , $2l$, $2R_1$, $2R_2$, and the diameter of the wire with insulation are 400, 40 mm, 20 mm, 40 mm, and 1 mm respectively. To fabricate this newly designed coil, a ~ 40 m-long wire should be prepared. Uniform and long round wires with larger cross section area of superconducting core is needed for generating larger magnetic field in the coil.

Further enhancement of J_c in IBS round wire is also expected. One of the most important parameter to increase J_c is the degree of texturing of superconducting grains. In this report, wires are drawn using mostly dies with circular holes, and a rotary swaging machine was used in the final processes. It was suggested in Ref. [63] that drawing wires using dies is preferred than swaging for increasing J_c . We used the rotary swaging machine in the final process to avoid breakage of the thin Cu/Ag-sheathed wires. The breakage of the wire using dies with smaller holes can be avoided by

inserting annealing process of the wire after several drawing processes. As described above, a higher degree of grain texturing is evaluated in the wire with largest J_c compared with the previous report. By improving the fabrication process, such as drawing wires exclusively using dies, may realize further texturing of the grains in the core. Next, uniform core shape over the entire length of the wire is also important. As shown in X-ray CT images in Figs. 4(c) and 4(f), slight sausaging of the core and unevenness of the interface between the Ag sheath and the core can be detected. Togano *et al.* reported that the smoothness of the interface between the sheath and the core in (Ba,K)Fe₂As₂ tape is significantly improved by using Ag-Sn binary alloy sheaths [64]. Using proper metal sheath, which is hard and stable against core material, uniform core shape in the wire can also be realized. Finally, quality of polycrystalline materials is also a key factor to reduce weak links between the grains and increase J_c . The condition of synthesis of polycrystalline sample directly affects the sample quality [42,48]. Kametani *et al.* reported that oxygen and water level should be significantly reduced in the synthesis environment [25]. Otherwise, insulating Ba-O network is formed at the grain boundaries. Actually, (Ba,K)Fe₂As₂ powder is degraded by accidental exposure to a little amount of air in the synthesis environment, as described above. Deterioration of qualities of (Ba,Na)Fe₂As₂ due to the exposure of small amount of oxygen or water is one of possible reasons for the difference of the quality between this work and the previous work as shown in Fig. 7(a). Reduction of chance for exposure to even a small amount of oxygen or water may be effective for avoiding the formation of weak links between superconducting grains.

Summary

We demonstrate the fabrication of small (Ba,A)Fe₂As₂ (A: Na, K) coils using 10 m-class long round wires, using PIT method. Coils are processed by using HIP technique after insulated round wires are wound on the bobbin. I_c of the whole coils using (Ba,Na)Fe₂As₂ and (Ba,K)Fe₂As₂ wires are 60 A and 66 A under the self-field, and generated magnetic fields at the center of the coil reach 2.6 kOe and 2.5 kOe, respectively. Furthermore, the largest transport J_c and I_c in (Ba,Na)Fe₂As₂ wires picked up from the coil reach 54 kAcm⁻² and 51.8 A at $T = 4.2$ K under a magnetic field of 100 kOe, respectively. This value exceeds the value of transport J_c of all previous IBS round wires. Texturing of grains in the superconducting core mainly plays an important role for the enhancement of transport J_c at high magnetic field, and higher quality of powders and higher densification of the core also contribute to that. For generating larger magnetic field in the coil, uniform and long round wires with larger cross sectional area of superconducting core is demanded. To increase J_c , improvements of fabrication conditions, selection of proper metal sheaths, and reduction of the chance of exposure of core materials to small amount of oxygen or water should be exercised.

Acknowledgements

This work was supported by a Grant-in-Aid for Scientific Research (A) (17H01141) from the Japan Society for the Promotion of Science (JSPS). A part of this study was performed at the High Field Laboratory for Superconducting Materials, Institute for Materials Research, Tohoku University (Project No. 20H0023). We are grateful to Dr. Ohtake and Prof. Suzuki in The University of Tokyo for performing X-ray CT imaging of (Ba,Na)Fe₂As₂ wires. A part of this work was supported by NIMS microstructural characterization platform (NMCP) as a program of "Nanotechnology Platform" of the Ministry of Education, Culture, Sports, Science and Technology (MEXT), Japan, Grant Number JPMXP09A20NM0131. We are grateful to Dr. Takenouchi in NMCP for performing X-ray CT imaging of (Ba,K)Fe₂As₂ wires.

References

- [1] Rotter M, Tegel M and Johrendt D 2008 *Phys. Rev. Lett.* **101** 107006
- [2] Sasmal K, Lv B, Lorenz B, Guloy A M, Chen F, Xue Y-Y and Chu C-W 2008 *Phys. Rev. Lett.* **101** 107007
- [3] Shirage P M, Miyazawa K, Kito H, Eisaki H and Iyo A 2008 *Appl. Phys. Express* **1** 081702
- [4] Zhao K, Liu Q Q, Wang X C, Deng Z, Lv Y X, Zhu J L, Li F Y and Jin C Q 2011 *Phys. Rev. B* **84** 184534
- [5] Avci S, Allred J M, Chmalssem O, Chung D Y, Rosenkranz S, Schlueter J A, Claus H, Daoud-Aladine A, Khalyavin D, Manuel P, Llobet A, Suchomel M R, Kanatzidis M G and Osborn R 2013 *Phys. Rev. B* **88** 094510
- [6] Cortes-Gil R and Clarke S J 2011 *Chem. Mater.* **23** 1009
- [7] Altarawneh M M, Collar K, Mielke C H, Ni N, Bud'ko S L and Canfield P C 2008 *Phys. Rev. B* **78** 220505(R)
- [8] Yuan H Q, Singleton J, Balakirev F F, Baily S A, Chen G F, Luo J L and Wang N L 2009 *Nature* **457** 565
- [9] Wang X-L, Ghorbani S R, Lee S-I, Dou S X, Lin C T, Johansen T H, Müller K-H, Cheng Z X, Peleckis G, Shabazi M, Qviller A J, Yurchenko V V, Sun G L and Sun D L 2010 *Phys. Rev. B* **82** 024525
- [10] Nagamatsu J, Nakagawa N, Muranaka T, Zenitani Y and Akimitsu J 2001 *Nature* **410** 63
- [11] Katase T, Ishimaru Y, Tsukamoto A, Hiramatsu H, Kamiya T, Tanabe K and Hosono H 2011 *Nat. Commun.* **2** 409
- [12] Nakajima Y, Tsuchiya Y, Taen T, Tamegai T, Okayasu S and Sasase M 2009 *Phys. Rev. B* **80** 012510
- [13] Ohtake F, Taen T, Pyon S, Tamegai T, Okayasu S, Kambara T and Kitamura H 2015 *Physica C* **518** 47
- [14] Tamegai T, Taen T, Yagyuda H, Tsuchiya Y, Mohan S, Taniguchi T, Nakajima Y, Okayasu S, Sasase M, Kitamura H, Murakami T, Kambara T and Kanai Y 2012 *Supercond. Sci. Technol.* **25** 084008
- [15] Pyon S, Taen T, Ohtake F, Tsuchiya Y, Inoue H, Akiyama H, Kajitani H, Koizumi N, Okayasu S and Tamegai T 2013 *Appl. Phys. Express* **6** 123101
- [16] Taen T, Ohtake F, Pyon S, Tamegai T and Kitamura H 2015 *Supercond. Sci. Technol.* **28** 085003
- [17] Ma Y 2012 *Supercond. Sci. Technol.* **25** 113001
- [18] Shimoyama J 2014 *Supercond. Sci. Technol.* **27** 044002
- [19] Ma Y 2015 *Physica C* **516** 17
- [20] Pallecchi I, Eisterer M, Malagoli A and Putti M 2015 *Supercond. Sci. Technol.* **28** 114005
- [21] Hosono H, Tanabe K, Takayam-Muromachi E, Kageyama H, Yamanaka S, Kumakura H,

- Nohara M, Hiramatsu H and Fujitsu S 2015 *Sci. Technol. Adv. Mater.* **16** 033503
- [22] Hosono H, Yamamoto A, Hiramatsu H and Ma Y 2018 *Mater. Today* **21** 278
- [23] Yao C and Ma Y 2019 *Supercond. Sci. Technol.* **32** 023002
- [24] Pyon S, Tamegai T, Takano K, Kajitani H, Koizumi N and Awaji S 2019 *J. Phys.: Conf. Ser.* **1293** 012042
- [25] Kametani F, Su Y F, Collantes Y, Pak C, Tarantini C, Larbalestier D and Hellstrom E 2020 *Appl. Phys. Express* **13** 113002
- [26] Gao Z, Togano K, Matsumoto A and Kumakura H 2014 *Sci. Rep.* **4** 4065
- [27] Lin H, Yao C, Zhang X, Zhang H, Wang D, Zhang Q, Ma Y W, Awaji S and Watanabe K 2014 *Sci. Rep.* **4** 4465
- [28] Zhang X, Yao C, Lin H, Cai Y, Chen Z, Li J, Dong C, Zhang Q, Wang D, Ma Y, Oguro H, Awaji S and Watanabe K 2014 *Appl. Phys. Lett.* **104** 202601
- [29] Gao Z, Togano K, Matsumoto A and Kumakura H 2015 *Supercond. Sci. Technol.* **28** 012001
- [30] Lin H, Yao C, Zhang X, Dong C, Zhang H, Wang D, Zhang Q, Ma Y, Awaji S, Watanabe K, Tian H and Li J 2014 *Sci. Rep.* **4** 6944
- [31] Huang H, Yao C, Dong C, Zhang X, Wang D, Cheng Z, Li J, Awaji S, Wen H and Ma Y 2018 *Supercond. Sci. Technol.* **31** 015017
- [32] Iyo A, Shinohara N, Tokiwa K, Ishida S, Tsuchiya Y, Ishii A, Asou T, Nishio T, Matsuzaki K, Takeshita N, Eisaki H and Yoshida Y 2015 *Supercond. Sci. Technol.* **28** 105007
- [33] Suwa T, Pyon S, Tamegai T and Awaji S 2018 *Appl. Phys. Express* **11** 063101
- [34] Suwa T, Pyon S, Tamegai T and Awaji S 2018 *J. Phys.: Conf. Ser.* **1054** 012045
- [35] Suwa T, Pyon S, Park A, Tamegai T, Tsuchiya Y, Awaji S and Watanabe K 2017 *J. Phys.: Conf. Ser.* **871** 012062
- [36] Imai S, Itou S, Ishida S, Tsuchiya Y, Iyo A, Eisaki H, Matsuzaki K, Nishio T and Yoshida Y 2019 *Sci. Rep.* **9** 13064
- [37] Weiss J D, Tarantini C, Jiang J, Kametani F, Polyanskii A A, Larbalestier D C and Hellstrom E E 2012 *Nat. Mat.* **11** 682
- [38] Pyon S, Tsuchiya Y, Inoue H, Kajitani H, Koizumi N, Awaji S, Watanabe K and Tamegai T 2014 *Supercond. Sci. Technol.* **27** 095002
- [39] Tamegai T, Pyon S, Tsuchiya Y, Inoue H, Koizumi N and Kajitani H 2015 *IEEE Trans. Appl. Supercond.* **25** 7300504
- [40] Pyon S, Yamasaki Y, Kajitani H, Koizumi N, Tsuchiya Y, Awaji S, Watanabe K and Tamegai T 2015 *Supercond. Sci. Technol.* **28** 125014
- [41] Hecher J, Baumgartner T, Weiss J D, Tarantini C, Yamamoto A, Jiang J, Hellstrom E E, Larbalestier D C and Eisterer M 2016 *Supercond. Sci. Technol.* **29** 025004
- [42] Pyon S, Suwa T, Park A, Kajitani H, Koizumi N, Tsuchiya Y, Awaji S, Watanabe K and Tamegai

- T 2016 *Supercond. Sci. Technol.* **29** 115002
- [43] Tamegai T, Suwa T, Pyon S, Kajitani H, Takano K, Koizumi N, Awaji S and Watanabe K 2017 *IOP Conf. Ser. Mater. Sci. Eng.* **279** 012028
- [44] Pyon S, Suwa T, Tamegai T, Takano K, Kajitani H, Koizumi N, Awaji S, Zhou N and Shi Z 2018 *Supercond. Sci. Technol.* **31** 055016
- [45] T. Tamegai, T. Suwa, D. Miyawaki, S. Pyon, K. Takano, H. Kajitani, N. Koizumi, and S. Awaji 2019 *IEEE Trans. Appl. Supercond.* **27** 7300605
- [46] D. Miyawaki, S. Pyon, T. Tamegai, S. Awaji, K. Takano, H. Kajitani, and N. Koizumi 2019 *J. Phys.: Conf. Ser.* **1293** 012043
- [47] Miyawaki D, Pyon S, Suwa T, Takano K, Kajitani H, Koizumi N, Awaji S and Tamegai T 2020 *Physica C* **568** 1353580
- [48] Pyon S, Miyawaki D, Tamegai T, Awaji S, Kito H, Ishida S and Yoshida Y 2020 *Supercond. Sci. Technol.* **33** 065001
- [49] Tamegai T, Pyon S, Miyawaki D, Kobayashi Y, Awaji S, Kito H, Ishida S, Yoshida Y, Takano K, Kajitani H and Koizumi N 2020 *Supercond. Sci. Technol.* **33** 104001
- [50] Yao C, Ma Y W, Zhang X P, Wang D L, Wang C L, Lin H and Zhang Q J 2013 *Appl. Phys. Lett.* **102** 082602
- [51] Yao C, Lin H, Zhang Q J, Wang D L, Dong C H, Ma Y W, Awaji S and Watanabe K 2015 *J. Appl. Phys.* **118** 203909
- [52] Zhu Y C, Wang D L, Zhu C D, Huang H, Xu Z T, Liu S F, Cheng Z and Ma Y W 2018 *Supercond. Sci. Technol.* **31** 06LT02
- [53] Imai S, Ishida S, Tsuchiya Y, Iyo A, Eisaki H, Nishio T and Yoshida Y 2020 *Supercond. Sci. Technol.* **33** 084011
- [54] Zhang X P, Oguro H, Yao C, Dong C H, Xu Z T, Wang D L, Awaji S, Watanabe K and Ma Y W 2017 *IEEE Trans. Appl. Supercond.* **27** 7300705
- [55] Wang D, Zhang Z, Zhang X, Jiang D, Dong C, Huang H, Chen W, Xu Q and Ma Y 2019 *Supercond. Sci. Technol.* **32** 04LT01
- [56] Zhang Z, Wang D, Liu F, Jiange D, Wei S, Wang Y, Gong L, Zhang X, Zhang Z, Liu H, Tian Chao, Ma Y and Xu Q 2020 *IEEE Trans. Appl. Supercond.* **30** 4602404
- [57] Zhang Z, Wang D, Wei S, Wang Y, Wang C, Zhang Z, Yao H, Zhang X, Liu F, Liu H, Ma Y and Xu Q 2021 *Supercond. Sci. Technol.* **34** 035021
- [58] Tamegai T, Miyawaki D, Pyon S, Wu W, Kajitani H, Koizumi N and Awaji S 2021 *IEEE Trans. Appl. Supercond.* **31** 7300505
- [59] Tanaka K, Okada M, Kumakura H, Kitaguchi H and Togano K 2002 *Physica C* **382** 203
- [60] Tanaka K, Kitaguchi H, Kumakura H, Yamada H, Hirakawa M and Okada M 2005 *Supercond. Sci. Technol.* **18** 678

- [61] G. F. Vander Voort, *Metallography: Principles and Practice*, Asm Intl, (1999).
- [62] D. B. Montgomery, *Solenoid Magnet Design*, Wiley-Interscience (1969).
- [63] Pyon S, Suwa T and Tamegai T 2017 *J. Phys.: Conf. Ser.* **871** 012060
- [64] Togano K, Gao Z, Matsumoto A, Kikuchi A and Kumakura H 2017 *Supercond. Sci. Technol.* **30** 015012

Table 1. Specifications of Cu-Ag-sheathed (Ba,A)Fe₂As₂ (A: Na, K) coils.

Structure	Parameters	(Ba,Na)Fe ₂ As ₂	(Ba,K)Fe ₂ As ₂
Wires	Diameter	1.0 mm	1.16 mm
	Length	~12.5 m	~10 m
	Filament number	Mono core	Mono core
Coils	Inner diameter ($2R_1$)	19 mm	19 mm
	Outer diameter ($2R_2$)	32 mm	35 mm
	Height ($2l$)	42 mm	25.5 mm
	Numbers of turns (N)	160	114
	Coil constant (calculated)	41 Oe/A	39 Oe/A
	Critical current (I_c)	60 A	66 A
	Generated magnetic field (H)	2.6 kOe	2.5 kOe
	Coil constant (measured)	43 Oe/A	38 Oe/A

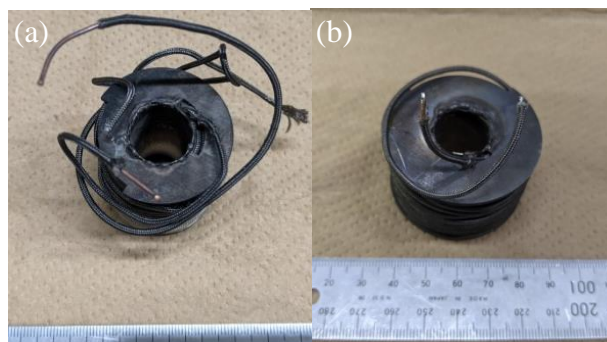


Figure 1. Optical photos of (a) the $(\text{Ba,Na})\text{Fe}_2\text{As}_2$ coil and (b) the $(\text{Ba,K})\text{Fe}_2\text{As}_2$ coil.

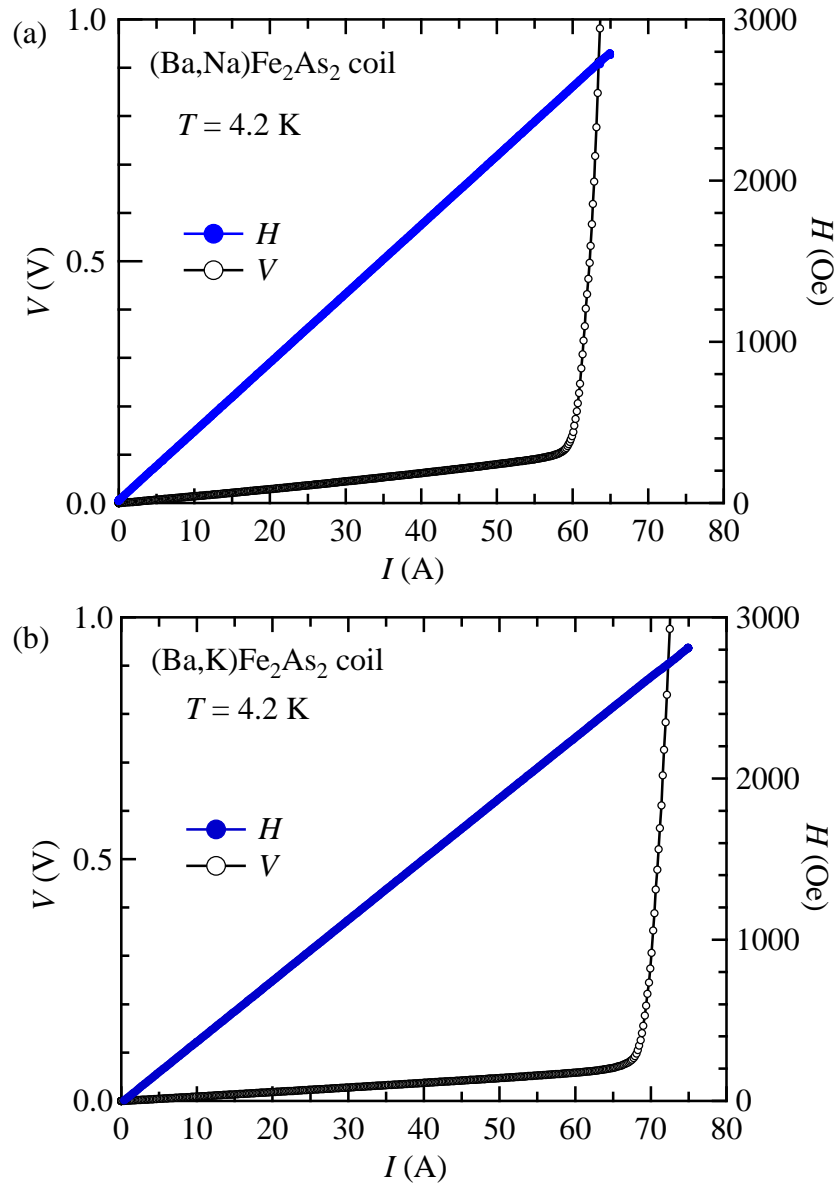


Figure 2. I - V characteristics and electric current dependence of generated magnetic field of (a) $(\text{Ba,Na})\text{Fe}_2\text{As}_2$ and (b) $(\text{Ba,K})\text{Fe}_2\text{As}_2$ coils. Measurements were performed at 4.2 K under the self-field.

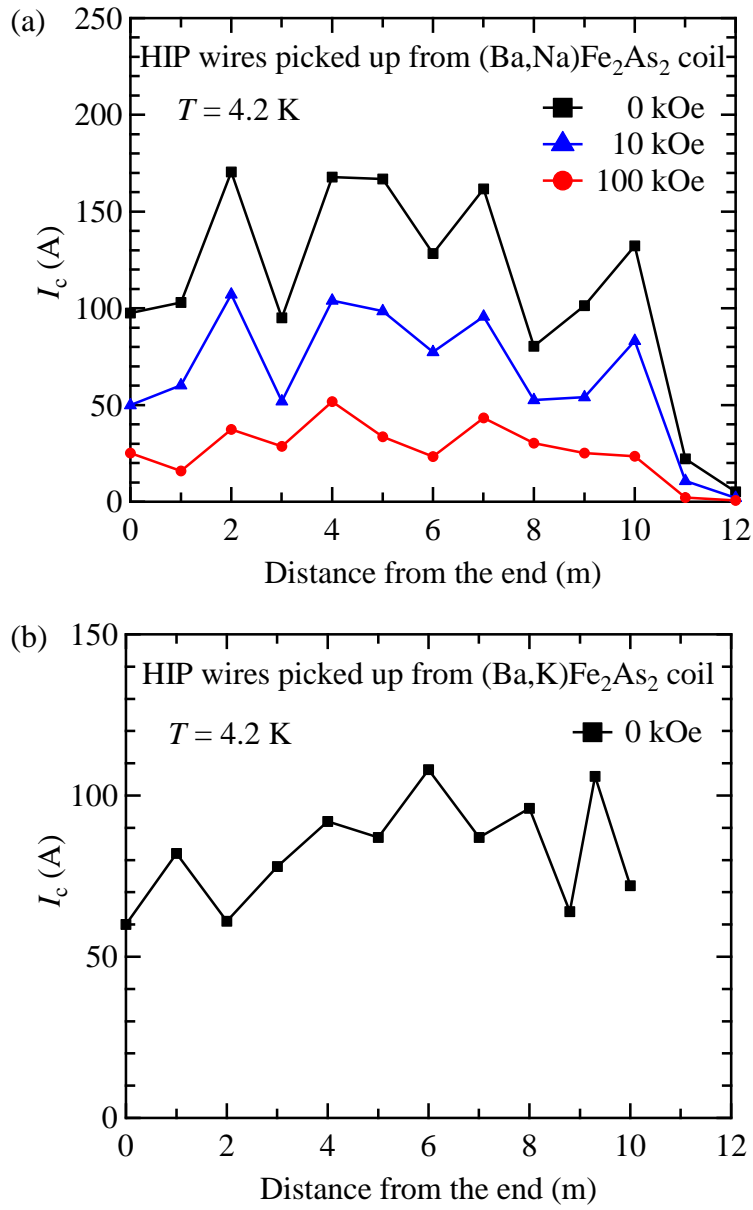


Figure 3. Transport I_c of short segments of wires picked up from (a) $(\text{Ba,Na})\text{Fe}_2\text{As}_2$ and (b) $(\text{Ba,K})\text{Fe}_2\text{As}_2$ coils. Measurements were performed at 4.2 K under several magnetic fields.

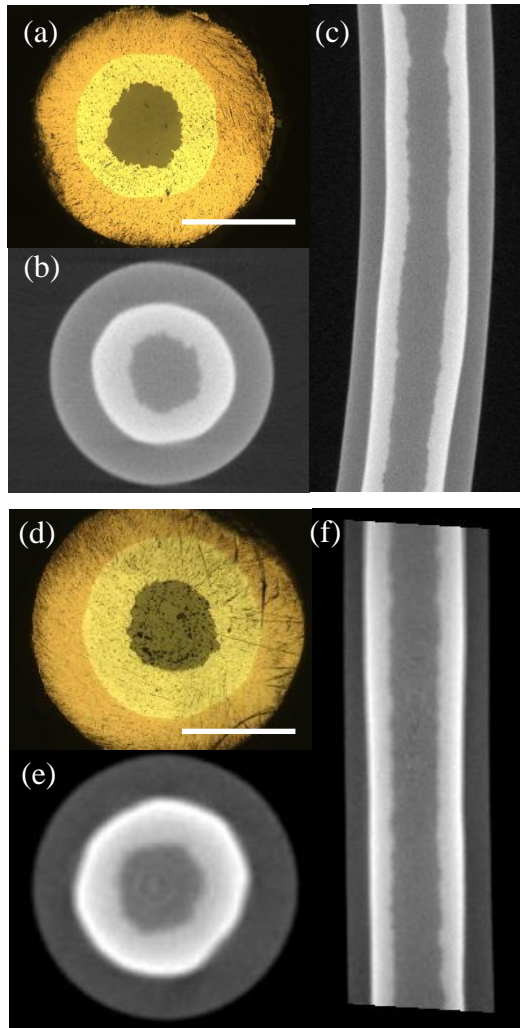


Figure 4. Optical micrographs and X-ray CT images of the transverse cross section of wires picked up from (a)-(b) $(\text{Ba,Na})\text{Fe}_2\text{As}_2$ coil and (d)-(e) $(\text{Ba,K})\text{Fe}_2\text{As}_2$ coil. White lines in (a) and (d) indicate 0.5 mm. X-ray CT images of the longitudinal cross section of wires picked up from (c) $(\text{Ba,Na})\text{Fe}_2\text{As}_2$ and (f) $(\text{Ba,K})\text{Fe}_2\text{As}_2$ coils.

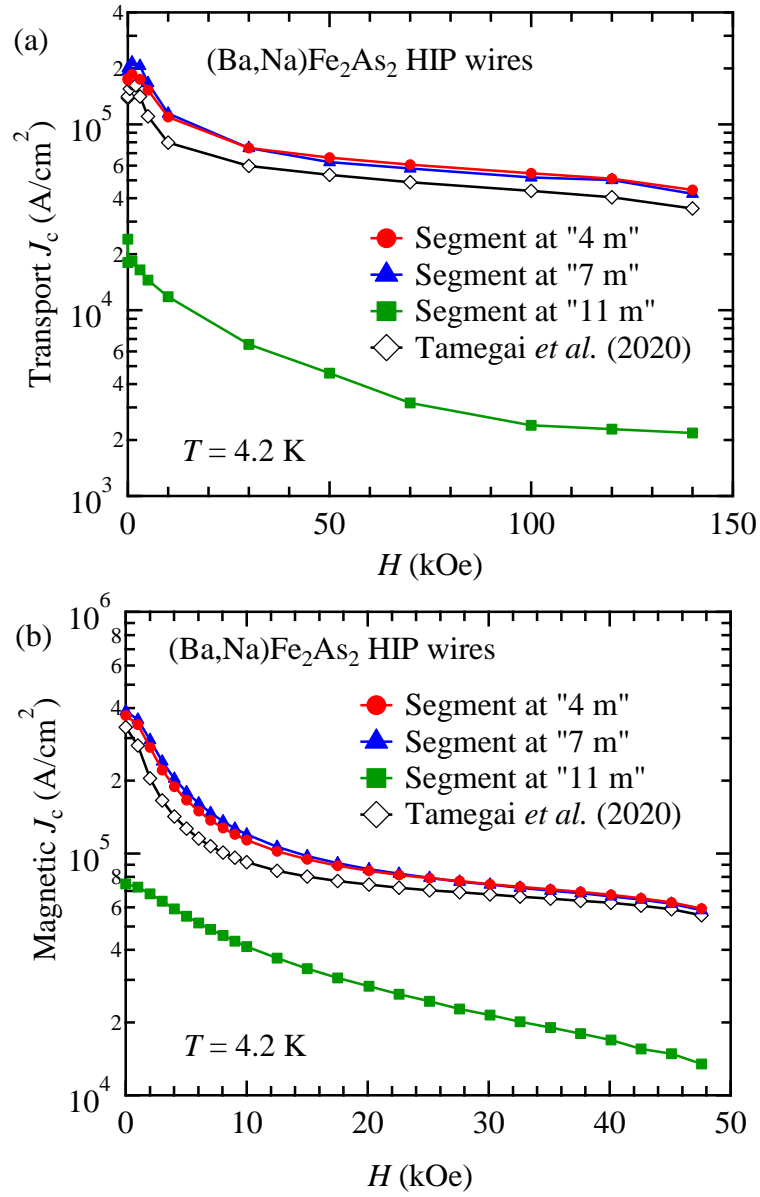


Figure 5. Magnetic field dependence of (a) transport J_c (I - V) and (b) magnetic J_c (M - H) at 4.2 K for the short segments picked up from the $(\text{Ba,Na})\text{Fe}_2\text{As}_2$ coil. Transport and magnetic J_c of the $(\text{Ba,Na})\text{Fe}_2\text{As}_2$ HIP wire from our previous study are also plotted for comparison [49].

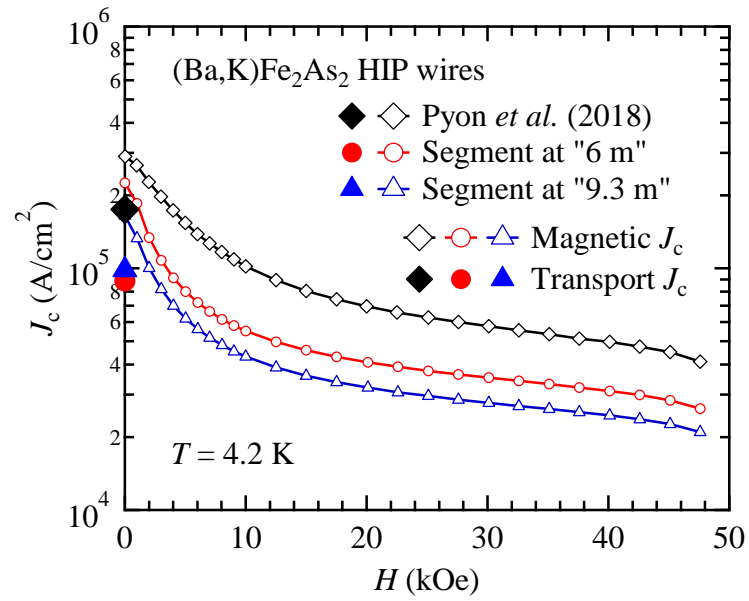


Figure 6. Magnetic field dependence of transport J_c (I - V) and magnetic J_c (M - H) at 4.2 K for the short segments picked up from the (Ba,K)Fe₂As₂ coil. Transport and magnetic J_c of the (Ba,K)Fe₂As₂ HIP wire from our previous study are also plotted for comparison [44].

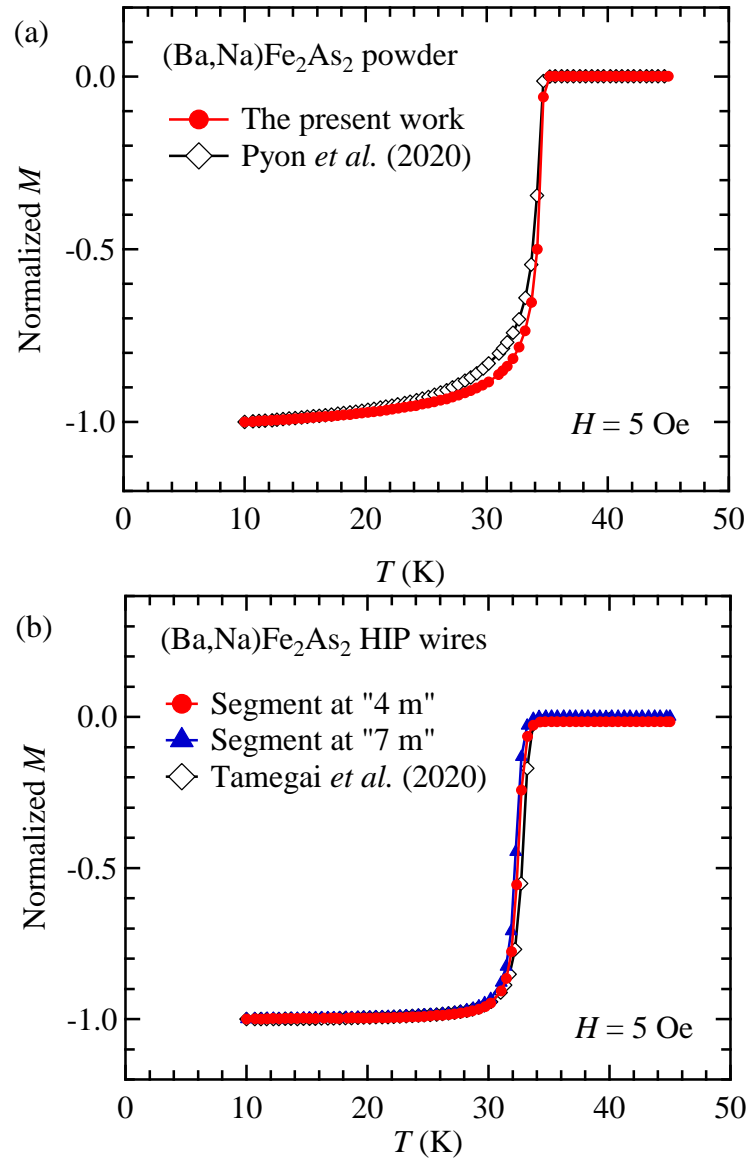


Figure 7. Temperature dependence of normalized magnetization at 5 Oe for (a) $(\text{Ba,Na})\text{Fe}_2\text{As}_2$ powders and (b) $(\text{Ba,Na})\text{Fe}_2\text{As}_2$ HIP wires. Data from our previous studies are also plotted for comparison [48,49].

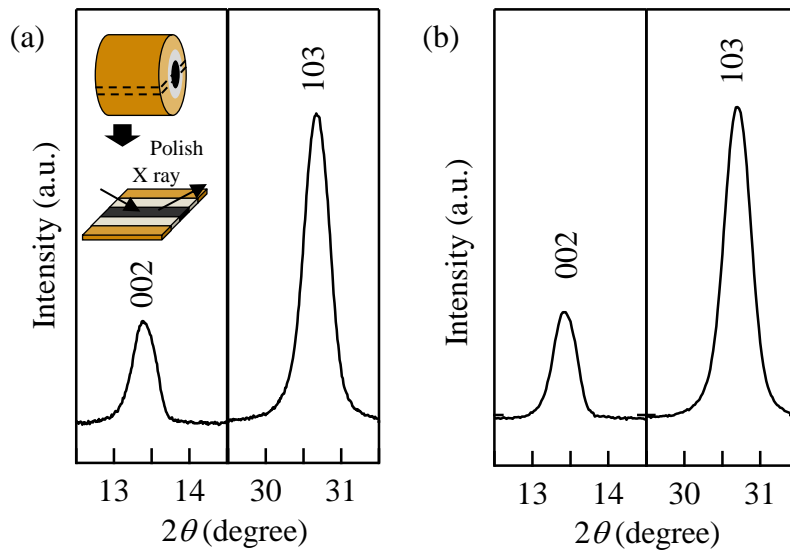


Figure 8. XRD patterns of (002) and (103) peaks for longitudinal cross section of the wire picked up from the $(\text{Ba,Na})\text{Fe}_2\text{As}_2$ coil at a distance (a) 4 m and (b) 1 m from the end of the wire.

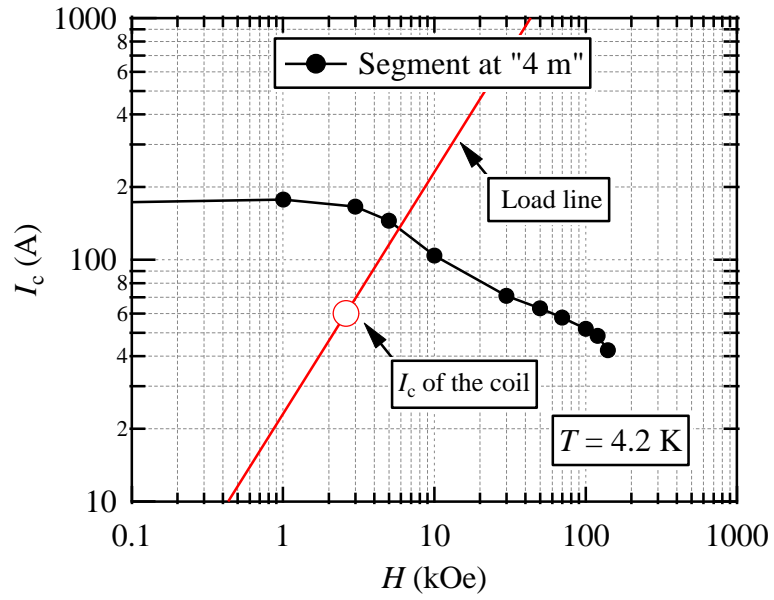


Figure 9. Load line of the $(\text{Ba},\text{Na})\text{Fe}_2\text{As}_2$ coil and the I_c - H curve of a short segment of the wire picked up from the coil at 4.2 K. The I_c of the $(\text{Ba},\text{Na})\text{Fe}_2\text{As}_2$ coil is indicated by an open circle.